Towards Interpretable and Efficient Attention: Compressing All by Contracting a Few

Qishuai Wen Zhiyuan Huang Chun-Guang Li

Beijing University of Posts and Telecommunications {wqs, huangzhiyuan, lichunguang}@bupt.edu.cn

Abstract

Attention mechanisms in Transformers have gained significant empirical success. Nonetheless, the optimization objectives underlying their forward pass are still unclear. Additionally, the quadratic complexity of self-attention is increasingly prohibitive. Unlike the prior work on addressing the interpretability or efficiency issue separately, we propose a unified optimization objective to alleviate both issues simultaneously. By unrolling the optimization over the objective, we derive an inherently interpretable and efficient attention mechanism, which compresses all tokens into low-dimensional structures by contracting a few representative tokens and then broadcasting the contractions back. This *Contract-and-Broadcast Self-Attention* (CBSA) mechanism can not only scale linearly but also generalize existing attention mechanisms as its special cases. Experiments further demonstrate comparable performance and even superior advantages of CBSA on several visual tasks. Code is available at this https URL.

1 Introduction

The Transformer architecture and attention mechanisms [1] have been widely applied across diverse areas, including computer vision [2, 3], natural language processing [4, 5], and scientific discovery [6]. Nonetheless, a series of puzzling phenomena have been uncovered in Transformers, such as the emergent segmentation properties [7], the in-context learning ability [8], the attention collapse [9, 10] and the extreme-token phenomena [11]. At the same time, the quadratic computational and memory complexity of self-attention with respect to the sequence length impedes its broader applications in real-time systems [12], as well as the processing of long documents [13] and high-resolution images [14].

In light of these challenges, it is crucial to demystify attention mechanisms and enhance the efficiency of self-attention. Over the past few years, remarkable advances have been made in addressing the interpretability or efficiency issue separately. On one hand, attention mechanisms can be interpreted as unrolling an optimization objective grounded in clustering [15], compression [16], or energy minimization [17]. These ante-hoc, inherently interpretable perspectives are generally considered more rigorous than post-hoc explanations [18]. On the other hand, numerous techniques have been proposed to alleviate the quadratic complexity of self-attention, including sparse attention [19], and linear attention [20].

However, a unified principle that jointly achieves interpretability and efficiency in self-attention remains largely unexplored. This leaves the design of efficient attention mostly heuristic and the theories behind interpretable attention less instructive. To bridge this gap, a recent work [21] introduced the the *maximal coding rate reduction* (MCR²) [22] objective but left several important questions unresolved. Their *token-statistic self-attention* (TSSA) adaptively scales feature channels based on their second moments, achieving high interpretability with linear computation complexity. Nevertheless, the channel attention [23, 24] manner of TSSA contrasts sharply with the spatial manner

of standard softmax attention [1]. Therefore, it remains an open question whether an interpretable framework can be developed to integrate attention mechanisms, ranging from full attention ¹ to linear attention and channel attention, that trade expression capacity for increased efficiency while revealing their fundamental differences.

In this paper, we propose a unified optimization objective to derive an inherently interpretable and efficient attention mechanism. To be specific, the proposed objective compresses input tokens into a union of subspaces by contracting a few representative tokens (abbreviated as *representatives*), making it more efficient than processing all tokens individually. By unrolling the optimization procedure over the objective, we derive our *Contract-and-Broadcast Self-Attention* (CBSA), which contracts a few representatives and broadcasts the contractions back to all input tokens, as illustrated in Fig. 1.

Given a fixed number of representatives, CBSA's computational and memory complexity scales linearly with the number of tokens. Moreover, varying the choice of representatives yields CBSA variants that trade efficiency for expression capacity, or vice versa. We demonstrate that: a) when each token serves as its own representative, CBSA recovers softmax attention; b) when representatives are orthogonal (e.g., the principal directions), CBSA reduces to linear attention; c) when representatives are orthogonal but fixed (i.e., input-agnostic), CBSA degenerates into channel attention. Our findings suggest that differences among these attention mechanisms arise from distinct choices of representatives, whose number and structure induce divergent patterns of information propagation.

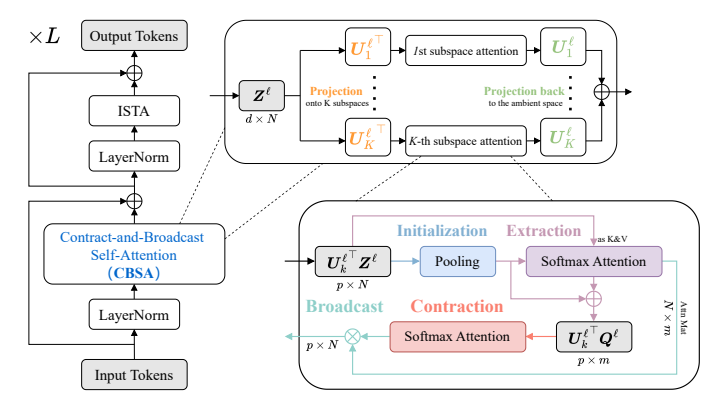


Figure 1: Contract-and-Broadcast Self-Attention (CBSA). Besides projection onto the subspace and back to the ambient space, our CBSA generally involves four steps: initialization, extraction, contraction, and broadcast. In Section 3.3, we show that different representative extraction strategies can simplify or fuse some of these steps, thereby leading to different attention mechanisms. A more easy to understand

Paper contributions

- 1. We propose a unified optimization objective that compresses all tokens by contracting a few representatives, thereby deriving an inherently interpretable and efficient attention mechanism.
- 2. By varying the choice of representatives, the derived mechanism, CBSA, generalizes existing attention mechanisms as special cases, reducing their fundamental differences to the number and structure of representatives.
- 3. We validate the interpretability and efficiency of CBSA through extensive experiments on visual tasks, highlighting its competitive or superior performance.

2 Notations and preliminaries

Given a positive integer n, we denote $[n] \doteq \{1, 2, \dots, n\}$. For $s \geq t$, we use $\mathcal{O}(s,t) \subseteq \mathbb{R}^{s \times t}$ to denote the set of $s \times t$ matrices with orthonormal columns, and $\mathcal{O}(s) \doteq \mathcal{O}(s,s)$ to denote the set of $s \times s$ orthogonal matrices. We denote an identity matrix of size n by \mathbf{I}_n , and similarly a zero square matrix by \mathbf{O}_n . Given a vector $\mathbf{v} \in \mathbb{R}^n$, let $\mathrm{Diag}(\mathbf{v}) \in \mathbb{R}^{n \times n}$ be a diagonal matrix with the elements of \mathbf{v} along the diagonal.

¹Softmax attention calculates all possible pairwise similarities among input tokens, i.e., it models a fully-connected digraph, and and is therefore also called full attention.

We use $Z \in \mathbb{R}^{d \times N}$ to denote a sequence of N input tokens represented in the d-dimensional ambient space, and specify these fed into the ℓ -th attention layer as Z^{ℓ} . The same holds for the tokens' representatives $Q \in \mathbb{R}^{d \times m}$, where m can be much smaller than N. The low-dimensional structure of representation is modeled as K incoherent p-dimensional subspaces spanned by orthonormal bases $U_{[K]} \doteq \{U_k \in \mathcal{O}(d,p)\}_{k=1}^K$, such that pK = d and $U_i^{\mathsf{T}}U_j = \mathbf{O}_p, \forall i \neq j$. For the i-th basis vector of U_k , we denote by u_{ki} . Similar to [16], we implement $U_{[K]}$ as learnable parameters in each attention layer, denoting the set modeled by the ℓ -th layer as $U_{[K]}^{\ell} = \{U_k^{\ell}\}_{k=1}^K$.

To quantify compactness, i.e., the extent to which the tokens are compressed towards the subspaces, we adopt the (lossy) *coding rate* [25], which measures how efficiently the token distribution can be covered by ϵ -balls under a given quantization precision $\epsilon > 0$. The coding rate of the input tokens in the ambient space is defined as:

$$R(\mathbf{Z}) \doteq \frac{1}{2} \log \det \left(\mathbf{I}_N + \frac{d}{N\epsilon^2} \mathbf{Z}^\top \mathbf{Z} \right),$$
 (1)

and similarly defined for the projections onto the k-th subspace as $R(U_k^{\top} Z)$.

3 Methods

3.1 Compressing all by contracting a few

Before presenting our proposed optimization objective, we start from a well-established learning objective grounded in compression, *maximal coding rate reduction* (MCR²) [22, 26], and streamline it by introducing representatives.

The MCR 2 objective aims to compress tokens into K subspaces while expanding them in the ambient space to learn compact and structured representation. Specifically, it quantifies both compression and expansion through the coding rate, and can be formulated as follows:

$$\max_{\mathbf{Z}} \Delta R(\mathbf{Z}) \doteq \underbrace{R(\mathbf{Z})}_{\text{expansion}} - \underbrace{R_c(\mathbf{Z} \mid \mathbf{U}_{[K]})}_{\text{compression}} \doteq R(\mathbf{Z}) - \sum_{k=1}^{K} R(\mathbf{U}_k^{\top} \mathbf{Z}). \tag{2}$$

By unrolling the optimization over the compression term of (2), Yu et al. [16] derived an inherently interpretable softmax attention mechanism called *multi-head subspace self-attention* (MSSA) (9), which also scales quadratically. This complexity essentially arises from the fact that (1) calculates the Gram matrix of tokens in order to compress them.²

Inspired by the scaling strategies built upon landmarks [28, 29, 30], in this paper, We propose to streamline the MCR² objective by compressing all input tokens through contracting a small number of *representatives* of them, resulting in a new objective that requires minor modifications to the compression term of (2):

$$\max_{\boldsymbol{Z}} R(\boldsymbol{Z}) - \sum_{k=1}^{K} R(\boldsymbol{U}_{k}^{\top} \boldsymbol{Q}) \quad \text{s.t. } \sum_{k=1}^{K} R(\boldsymbol{U}_{k}^{\top} \boldsymbol{Q}) = \sum_{k=1}^{K} R(\boldsymbol{U}_{k}^{\top} \boldsymbol{Z}), \tag{3}$$

where the optimization variable involves only input tokens Z, as representatives Q is extracted from it.³ When the constraint of (3) holds, (3) is equivalent to (2) but with much higher efficiency, because the number of representatives (e.g., m = p = d/K) is usually far smaller.

Relaxation and regularization of (3). As the equality constraint of (3) is overly restrictive in practice, we relax it by introducing a tolerance parameter τ , which bounds the absolute difference between the two coding rates within each subspace, resulting in the following inequality constraints:

$$\left| R(\boldsymbol{U}_{k}^{\top}\boldsymbol{Q}) - R(\boldsymbol{U}_{k}^{\top}\boldsymbol{Z}) \right| \le \tau, \ \forall k \in [K].$$
(4)

²By the commutative property of the coding rate [25], the Gram matrix can be equivalently replaced by the covariance matrix, which directly addresses the quadratic complexity [27, 21]. However, as discussed in the introduction, this leads to an invertible degeneration to channel attention.

³Note that the representatives are not necessarily a subset of the input tokens; rather, they resemble the cluster centroids in *K*-means and are continuously determined, rather than discretely selected from the inputs.

As a result, contracting the representatives via (3) ensures that the input tokens are correspondingly compressed in most cases, despite a potential significant gap between their coding rates. Additionally, note that the coding rate is invariant under any orthogonal transformation [22]. In extreme cases, if no additional structural constraint linking representatives to input tokens is imposed, the representatives could even be orthogonal to all input tokens, while still yielding identical coding rates. Therefore, we regularize the relaxed constraints (4) through a reconstruction term, such that the representatives can be expressed as linear combinations of the input tokens.

Eventually, the optimization objective that our subsequent derivations rely on is formulated as:

$$\min_{\boldsymbol{Z}} \sum_{k=1}^{K} R(\boldsymbol{U}_{k}^{\top} \boldsymbol{Q})$$
s.t. $\left| R(\boldsymbol{U}_{k}^{\top} \boldsymbol{Q}) - R(\boldsymbol{U}_{k}^{\top} \boldsymbol{Z}) \right| \leq \tau, \ \boldsymbol{U}_{k}^{\top} \boldsymbol{Q} = \boldsymbol{U}_{k}^{\top} \boldsymbol{Z} \boldsymbol{A}_{k}, \ \forall k \in [K],$ (5)

where $\{A_k \in \mathbb{R}^{N \times m}\}_{k=1}^K$ are the coefficient matrices over the dictionaries $\{U_k^\top Z \in \mathbb{R}^{p \times N}\}_{k=1}^K$. Following [16], we optimize the expansion term R(Z) in alternation with the compression term via a feed-forward module named ISTA, and thus have omitted it in (5).

3.2 Contract-and-Broadcast Self-Attention

In this subsection, we derive our inherently interpretable and efficient attention mechanism by translating the gradient-based optimization procedure over (5) into forward-pass operations.

Representative initialization and extraction. According to [31], an inherently interpretable cross-attention mechanism based on MCR², called *multi-head subspace cross-attention* (MSCA), can be interpreted as aligning the coding rates of its query and key/value ⁵. Therefore, we begin with an initial guess of the representatives as the query of MSCA, and take the input tokens as the key and value to extract representatives that satisfy the constraints in (5). In addition, the attention matrices in the attention heads of MSCA ⁶ directly serve as the coefficient matrices in (5), since the query is updated as linear combinations of the key. Following [30], we employ a pooling-based strategy for representative initialization.⁷ More details are deferred to the Appendix A, as our primary focus here is on the subsequent derivation.

Representative contraction and contraction broadcast. Having initialized the representatives via pooling the input tokens and extracted those satisfying the constraints of (5) via MSCA, we move on to taking a gradient descent step on the objective of (5):

$$Z \leftarrow Z - \eta \nabla_{Z} \left(\sum_{k=1}^{K} R(U_{k}^{\top} Q) \right) = Z - \kappa \operatorname{CBSA}(Z \mid U_{[K]}),$$
 (6)

$$CBSA(\boldsymbol{Z} \mid \boldsymbol{U}_{[K]}) \doteq \sum_{k=1}^{K} \boldsymbol{U}_{k} \underbrace{\boldsymbol{U}_{k}^{\top} \boldsymbol{Q} \left(\mathbf{I}_{m} + \frac{p}{m\epsilon^{2}} (\boldsymbol{U}_{k}^{\top} \boldsymbol{Q})^{\top} (\boldsymbol{U}_{k}^{\top} \boldsymbol{Q}) \right)^{-1}}_{Contraction, \propto \nabla_{\boldsymbol{Q}} R(\boldsymbol{U}_{k}^{\top} \boldsymbol{Q})} \underbrace{\boldsymbol{A}_{k}^{\top}}_{Broadcast},$$
(7)

where η denotes the original step size of the gradient descent update, and the step-size κ is introduced to absorb the gradient coefficient for notational simplicity. The contraction term in (7) is named so because it is proportional to the gradient of the representatives' coding rate with respect to themselves, which specifies the contraction direction (abbreviated as contractions) of them. The broadcast term in (7), an $m \times N$ matrix encoding the linear relationships between representatives and input tokens, serves to broadcast the contractions back to all input tokens.

⁴In Fig. 6, we observe that although the gap (i.e., τ) is significant, the trends of the two coding rates still closely echo each other. We thus do not deliberately constrain the value of τ .

⁵In the context of inherently interpretable attention mechanisms based on MCR², the query, key, and value coincide in self-attention, while the key and value coincide in cross-attention. The reason for this will become clear in the following derivation of CBSA

⁶That is, $A_k = \operatorname{softmax} ((U_k^\top Z)^\top (U_k^\top Q_0))$, where Q_0 denotes the initialized representatives.

⁷Another intuitive choice is to initialize them as learnable parameters, as in [32]. However, we find that this strategy suffers from a low-rank problem, which is discussed in the Appendix A.

To reduce the computational overhead of the contraction step, we adopt [16, Approximation 4], which replaces the matrix inverse with a Gram matrix followed by a softmax (i.e., an attention matrix), yielding the CBSA operator implemented in our Transformer models:⁸

$$CBSA(\boldsymbol{Z} \mid \boldsymbol{U}_{[K]}) \doteq \sum_{k=1}^{K} \boldsymbol{U}_{k} \underbrace{\boldsymbol{U}_{k}^{\top} \boldsymbol{Q} \operatorname{softmax} \left((\boldsymbol{U}_{k}^{\top} \boldsymbol{Q})^{\top} (\boldsymbol{U}_{k}^{\top} \boldsymbol{Q}) \right)}_{Contraction \text{ via self-attention}} \underbrace{\boldsymbol{A}_{k}^{\top}}_{Broadcast}.$$
(8)

The self-attention operation above corresponds to softmax attention, except that the linear projections for query, key, and value are all replaced by the subspace basis, i.e., $\boldsymbol{W}^{\mathrm{q}} = \boldsymbol{W}^{k} = \boldsymbol{W}^{v} = \boldsymbol{U}_{k}^{\mathsf{T}}$. By default, we adopt this simplified version (8) in our *Contract-and-Broadcast Transformer* (CBT), as illustrated in Fig. 1. Nonetheless, as will be shown in the next subsection, it is the rigorous prototype (7) that exposes the fundamental connections among different attention mechanisms.

Overview and complexity analysis of CBSA and CBT. Our CBSA efficiently processes input tokens through the following steps: it projects input tokens into subspaces (i.e., attention heads parameterized by $U_{[K]}$), initializes representatives via pooling, extracts representatives via cross-attention, contracts them via self-attention, and broadcasts the contractions back to all tokens according to the attention matrices computed in the extraction step. For an overall interpretability, we adopt ISTA [16] as the feedforward block, as it optimizes the expansion term omitted from (5). We present the computational complexities of CBSA and its sub-operations in Table 1, and compare the FLOPs of different attention mechanisms in Fig. 2. Provided N > 2d/H = 2p (typically 128 in Transformers), the

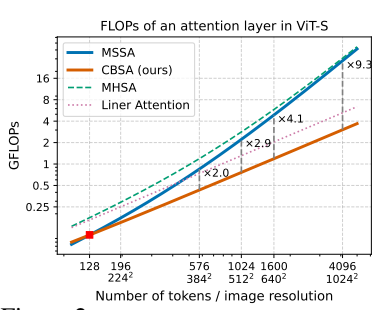


Figure 2: FLOPs of a single attention layer, with d=384, H=6, and a patch size of 16×16 .

FLOPs of CBSA are lower than those of MSSA. Comparisons with more modules, such as MHSA and MLP, can be found in Fig. 9.

Table 1: Computational complexities. By default, we set m = p = d/H, where H = K denotes the number of attention heads (interpreted as subspaces in our case). The complexity of each sub-operation is computed by summing the costs across all heads. It is worth noting that the projection operations, which are essential to almost all attention mechanisms, bottlenecks the overall complexity always over $\mathcal{O}(Nd^2)$.

$\Omega({\rm MSSA})$	$\Omega(\mathrm{CBSA})$	$\begin{array}{cc} \text{sub-operations of CBSA} \\ \Omega(\text{extraction}) / \Omega(\text{broadcast}) & \Omega(\text{contraction}) & \Omega(\text{projection}) \end{array}$				
$2Nd^2 + 2N^2d$	$2Nd^2 + 3Nmd + 2m^2d$	Nmd	m^2d	Nd^2		

3.3 Variants of CBSA

In this subsection, we demonstrate that specifying different sets of representatives or their extraction strategies derives variants of CBSA that can be categorized as existing attention mechanisms. In these variants, the initialization, extraction, contraction, and broadcast steps of CBSA may not be explicitly observed, as some steps are simplified or fused together due to their specific number and structure of the representatives.

Agent Attention [30] as CBSA variant. As illustrated in Fig. 3, if we remove the contraction step of CBSA, it derives the Agent Attention, which was proposed to be a generalized form of linear attention. Actually, we argue that, in this case, the contraction step is not removed but fused into the extraction step, since most of the extraction's purpose already achieved by pooling the input tokens.

We previously extract representatives satisfying the relaxed constraints in (5) via MSCA with an initial guess, yielding an approximate numerical solution to the constraints of the original problem (3). Beyond this, closed-form optimal solutions ¹⁰ also exist, which can either improve interpretability and efficiency or enhance the expressive capacity of the resulting mechanism.

⁸Note that the scaling factor and possible sign inversion introduced by this approximation are absorbed by κ again, which is implemented as a learnable parameter in the model.

⁹Since query, key, and value coincide in CBSA (8), the broadcast matrix in Agent Attention can be obtained directly from the extraction (i.e., cross-attention) step.

¹⁰That is, the representatives that not only have the same coding rate as the input tokens but also possess an explicit coefficient matrix allowing them to be linearly expressed by the input tokens.

Softmax attention as CBSA variant. Apparently, the input tokens themselves satisfy the constraints and thus can be directly used as the representatives, i.e., Q = Z, m = N. In this case, we say the input tokens are *self-expressed* [33], since data samples are linearly represented over a dictionary composed of themselves. Then we can take a trivial solution for the regularization term where all coefficient matrices reduces to identity matrices. Substituting them into (8) yields the following operator, known as MSSA in white-box transformers [16]:

$$MSSA(\boldsymbol{Z} \mid \boldsymbol{U}_{[K]}) \doteq \sum_{k=1}^{K} \boldsymbol{U}_{k} \underbrace{\boldsymbol{U}_{k}^{\top} \boldsymbol{Z}}_{\text{v.s. } \boldsymbol{W}^{v} \boldsymbol{Z}} \underbrace{\text{softmax} \left((\boldsymbol{U}_{k}^{\top} \boldsymbol{Z})^{\top} (\boldsymbol{U}_{k}^{\top} \boldsymbol{Z}) \right)}_{\text{v.s. } \text{softmax} \left((\boldsymbol{W}^{k} \boldsymbol{Z})^{\top} (\boldsymbol{W}^{q} \boldsymbol{Z}) \right)}.$$
(9)

Linear attention as CBSA variant. To analyze the case of orthogonal representatives, we start with the canonical choice: the principal directions of input tokens, along which projections yield the principal components. Specifically, We perform singular value decomposition (SVD) on the token projection within each subspace:

$$\boldsymbol{U}_{k}^{\top} \boldsymbol{Z} = \boldsymbol{L}_{k} \boldsymbol{\Sigma}_{k} \boldsymbol{R}_{k}^{\top}, \ \forall k \in [K], \tag{10}$$

where $L_k \in \mathcal{O}(p)$, $R_k \in \mathcal{O}(N,p)$, and Σ_k is a $p \times p$ diagonal matrix of singular values. The columns of L_k are known as the principal directions. Then, by right multiplying both sides by R_k , we have:

$$\boldsymbol{U}_{k}^{\top} \boldsymbol{Z} \boldsymbol{R}_{k} = \boldsymbol{L}_{k} \boldsymbol{\Sigma}_{k} \boldsymbol{R}_{k}^{\top} \boldsymbol{R}_{k} = \boldsymbol{L}_{k} \boldsymbol{\Sigma}_{k}, \ \forall k \in [K],$$
(11)

By comparing (10) with the constraints in (5), we let $U_k^{\top}Q = L_k\Sigma_k$, $A_k = R_k$. Substituting them into (7) leads to the following operation:

$$\sum_{k=1}^{K} \boldsymbol{U}_{k} \underbrace{F\left((\boldsymbol{U}_{k}^{\top} \boldsymbol{Z})(\boldsymbol{U}_{k}^{\top} \boldsymbol{Z})^{\top}\right)}_{\text{v.s. } \boldsymbol{W}^{v} \boldsymbol{Z} \boldsymbol{\phi}(\boldsymbol{W}^{k} \boldsymbol{Z})^{\top}} \underbrace{\boldsymbol{U}_{k}^{\top} \boldsymbol{Z}}_{\text{v.s. } \boldsymbol{\phi}(\boldsymbol{W}^{q} \boldsymbol{Z})}, \tag{12}$$

where F is a function defined on the spectrum of a positive semi-definite matrix which applies $f(\lambda_i) = \epsilon^2/(\epsilon^2 + \lambda_i)$ to the eigenvalues $\{\lambda_i\}_{i=1}^p$ of the covariance matrix of the token projections. In Appendix B, we prove that this result holds for any set of orthogonal representatives. We find that (12) conceptually resembles linear attention, as it also factorizes the $N \times N$ attention matrix and multiplies the key and value first to linearize the computational complexity. I^2

Channel attention as CBSA variant. If we assume that the subspace bases U_k always correspond to the principal directions of any input token set, which is practically impossible but simplifies the operations, the representatives can be fixed as U_k (i.e., $Q = [U_1^\top \dots U_K^\top]^\top$), and are thus orthogonal and input-agnostic. Then (12) is reduced to:

$$\sum_{k=1}^{K} \boldsymbol{U}_{k} \boldsymbol{D}_{k} \boldsymbol{U}_{k}^{\top} \boldsymbol{Z}, \ \boldsymbol{D}_{k} \doteq \operatorname{Diag}\left(\left[f\left((\boldsymbol{u}_{ki}^{\top} \boldsymbol{Z})(\boldsymbol{u}_{ki}^{\top} \boldsymbol{Z})^{\top}\right)\right]_{i=1}^{p}\right), \tag{13}$$

which corresponds to TSSA [21] without exploiting token-to-subspace membership. In (13), the feature channels are adaptively scaled based on the second moment of the token projections, whereas typical channel attention mechanisms employ an MLP to predict the scaling factors.

Besides a graph perspective, the above findings can also be interpreted from a dictionary learning perspective, by treating the representatives as atoms of a dictionary. When the representatives are orthogonal and fixed, they form a complete dictionary; when they are orthogonal but input-dependent, they resemble a submatrix of an overcomplete dictionary in compressed sensing [34]. When the input tokens themselves serve as representatives, they constitute a self-expressive dictionary [33].

 $^{^{11}}$ As f is monotonically decreasing, (12) preserves the principle directions (i.e., representatives) with large variance while suppressing those with vanishing variance [27].

¹²In fact, linear attention is more expressive than (12), since $(\boldsymbol{U}_k^{\top}\boldsymbol{Z})(\boldsymbol{U}_k^{\top}\boldsymbol{Z})^{\top}$ is symmetric, whereas $(\boldsymbol{W}^v\boldsymbol{Z})(\boldsymbol{W}^k\boldsymbol{Z})^{\top}$ is generally not. How to interpret the transition from such symmetric attention to their asymmetric counterparts remains largely unexplored. For now, one can view it as overparameterization.

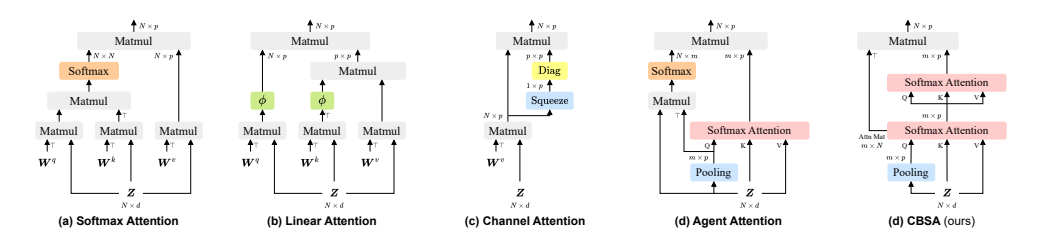


Figure 3: Overview of different attention mechanisms. Zoom in for better view.

4 Experiments

In this section, we evaluate the interpretability and efficiency of the proposed inherently interpretable attention, CBSA, and the CBT models built upon it. Since natural images often lie on low-dimensional subspaces [35, 36], we focus on classical visual tasks such as image classification and semantic segmentation, where higher resolutions generally lead to better accuracy [37, 38]. Experimental results copied from their original work will be in grey color, otherwise the results will be reproduced by us in varied settings for fair comparisons.

Baseline and training configuration. We primarily compare CBSA with previous interpretable attention mechanisms grounded in MCR², along with pioneering and classical Transformer-based models. Table 2 summarizes these baselines with brief descriptions. Results directly copied from the original papers are shown in grey, while the others are reproduced by us under varied settings for fair comparisons. Unless otherwise specified, the training configuration follows that of the baselines, with detailed information provided in Appendix C.

Implementation detail. We over-parameterize the projection step that maps tokens back to the ambient space, where the projection matrix should theoretically be $U_{[K]}$, by a set of independently learned parameter matrices. This trick is also adopted by MSSA [16] and TSSA [21], and its impact has been investigated in [39]. In short, although this relaxation compromises the theoretical rigor, it is crucial for achieving better accuracy. In addition, the positive scalar κ in (6) is implemented as a learnable parameter without constraining its sign. This allows the model to flexibly choose between compression and de-compression. We provide the PyTorch implementation in Appendix D.

Table 2: **Summary of baselines.** Note that these methods are not necessarily limited to the task listed behind, our description here only reflects their usages in this paper.

Method	Attention mechanism	Complexity	Interpretable	Task
ViT [2]	MHSA (softmax attention)	quadratic	×	image classification
CRATE [16]	MSSA (softmax attention)	quadratic	✓	image classification
ToST [21]	TSSA (channel attention)	linear	✓	image classification
Agent Attention [30]	Agent Attention (linear attention)	linear	×	image classification
Segmenter [40]	MHSA	quadratic	×	semantic segmentation
DEPICT [31]	MSSA / MSCA (cross-attention)	quadratic / linear	✓	semantic segmentation

4.1 Advantages enabled by interpretability

In this subsection, we show some superior advantages of CBSA over non-interpretable attention mechanisms. The most essential one is its interpretability, which further induces other desirable properties such as robustness and emergent segmentation.

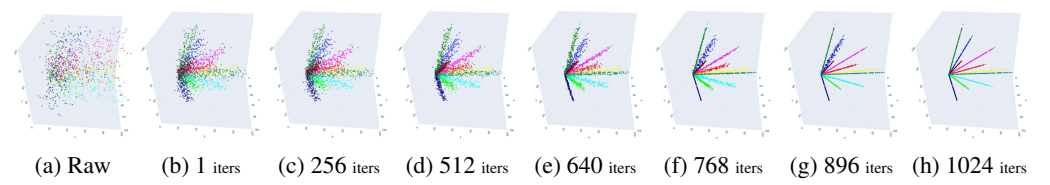


Figure 4: Compact and structured representation. There are 10 classes in total and each class has 200 samples.

Learning compact and structured representation. Similar to MCR², our optimization objective (3) also aims to learn compact and structured representations, i.e., compressing input tokens towards low-dimensional structures such as a mixture of subspaces. To verify that CBSA can achieve this goal, we evaluate the linear-attention-like variant of CBSA (12) on synthetic data. As illustrated in Fig. 4, we emulate image tokens as points in a 3-dimensional space, where ground-truth clustering memberships are indicated by color, and apply (12) iteratively. Since the operation is directly performed in the ambient space and no parameterized subspace is required, this procedure can be executed in a purely forward manner under supervision.

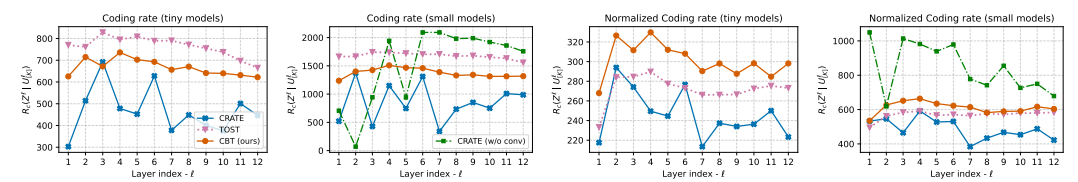


Figure 5: We measure the compression term of (2) across layers in different models.

Compressing all by contracting a few. To verify our interpretation that CBSA compresses all tokens through the contraction of a few representatives, we conduct two-fold experiments showing that the input tokens are indeed compressed and that this compression is driven by the contraction of the representatives. In Fig. 5, we measure the compression term of (2) using the coding rate (1) and its normalized variant ¹³. The normalized coding rate is invariant to in-place scaling and therefore captures only the angular compression. We observe two pieces of evidence supporting the compression interpretation: 1) representation compactness in the last layer, measured by the coding rate in Fig. 5, positively correlates with classification accuracy in Table 3; 2) in nearly all models, the latter half of the layers exhibit consecutive compression. We also identify a decompression phenomenon in the earlier layers, which we regard as a "known unknown" requiring further investigation. In Fig. 6, we measure the "compressed volume" of input tokens and their representatives separately after being processed by CBSA (without projecting back to the ambient space, so the results are reported per subspace). We observe that the compressed volumes of the two exhibit highly similar trends across most subspaces.

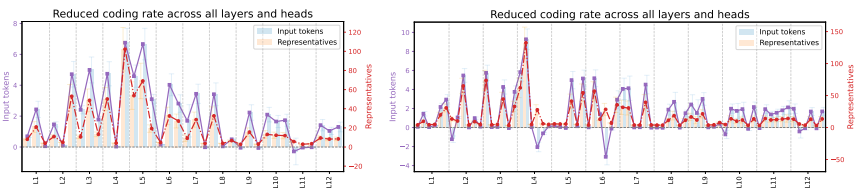


Figure 6: We measure the compressed volume of input tokens and their representatives using the reduced coding rate across all heads of a model. Results from CBT-T/S are presented here, those of CBT-B/L can be found in Fig. 10. Note that we set $\kappa = 1$ to exclude the de-compression cases observed in Fig. 5.

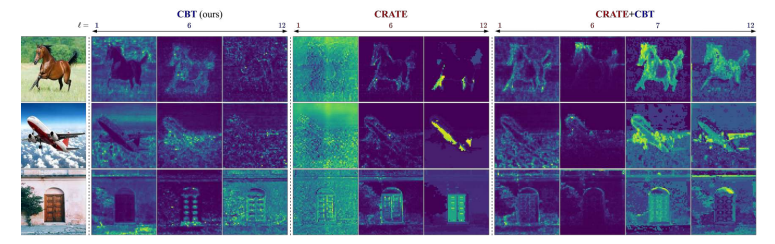


Figure 7: [CLS] attention map. We use $A_k A_k^{\top} \in \mathbb{R}^{N \times N}$ to empirically approximate the full attention matrix. Based on this, we extract the attention map of the [CLS] token from the early, middle, and late layers of CBT, CRATE, and their hybrid model.

Emergent segmentation properties. Owing to MSSA, segmentation properties emerge in CRATE with merely standard supervised classification training [41]. In Fig. 7, we visualize the attention map of the [CLS] token across different models. We observe that CBT attends to more semantically meaningful regions in the early layers compared to CRATE, but its segmentation properties do not persist in subsequent layers. To address this, we construct a hybrid model, termed CRATE+CBT,

¹³All input tokens are first normalized to unit vectors before calculating the normalized coding rate.

where the first half of the attention layers employ MSSA and the latter half employ CBSA. In this hybrid model, segmentation properties not only emerge in the very first layer, but are also progressively enhanced in the following layers, rather than fading as in CBT. Qualitative results supporting this conclusion can be found in Appendix C.

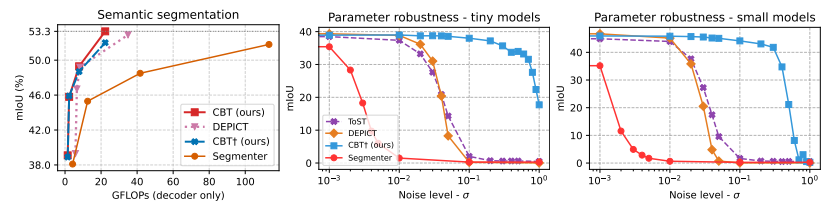


Figure 8: **Semantic segmentation on ADE20K.** † indicates that CBSA implemented rigorously, i.e., without the overparameterization trick. All results above are evaluated on the ADE20K validation set. *Leftmost panel:* The dotted horizontal line marks the best result. *Right two panels:* Random Gaussian noise with zero mean and standard deviation σ is independently added to each parameter of the attention layers in the decoder.

Robustness under parameter perturbation. As CBSA models low-dimensional subspaces via their attention heads, with parameter matrices corresponding to subspace bases, perturbing these basis vectors with relatively small noise does not significantly alter the subspaces they span [31]. Consequently, CBSA exhibits extreme robustness to parameter perturbations, whereas the black-box method Segmenter [40] collapses under the same perturbations, as illustrated in the right two panels of Fig. 8.

Table 3: Image classification on ImageNet-1K. The models are trained on images of resolution 224×224 with a patch size of 16. Note that the CBT models and ViT employ convolutional embedding layers, whereas the CRATE models use linear embeddings.

Datasets	CBT-T(iny)	CBT-S(mall)	CBT-B(ase)	CBT-L(arge)	CRATE-B	CRATE-L ViT-S
# parameters FLOPs	1.8M 1.1G	6.7M 4.0G	25.7M 15.1G	83.1M 47.3G	22.8M 12.6G	77.6M 22.1M 43.3G 9.8G
ImageNet-1K	63.2	71.4	73.4	74.4	70.8	71.3 72.4
CIFAR10 CIFAR100 Oxford Flowers-102 Oxford-IIIT-Pets	94.8 76.5 88.4 86.8	96.3 80.4 91.7 91.6	96.7 82.0 93.6 92.6	97.3 83.4 93.9 92.9	96.8 82.7 88.7 85.3	97.2 83.6 83.2 88.3 87.4 97.2 88.5 88.5 88.6

Table 4: **Fair comparisons on ImageNet-1K.** All models employ convolutional embedding layers and ISTA feedforward blocks. Their only difference lies in the attention mechanism. Specially, the Agent models do not follow the original implementation in [30]; instead, they are implemented as CBSA without the contraction step, as derived in Section 3.3.

ImageNet-1K	CBSA-T	CBSA-S TSSA-T	TSSA-S MSSA-T	MSSA-S Agent-T	Agent-S
# pairwise similarities	0.53M	1.1M 0.45M	0.91M 1.4M	2.8M 0.52M	1.0M
Top 1 accuracy	63.2	71.4 61.2	68.5 64.7	72.1 63.8	71.8

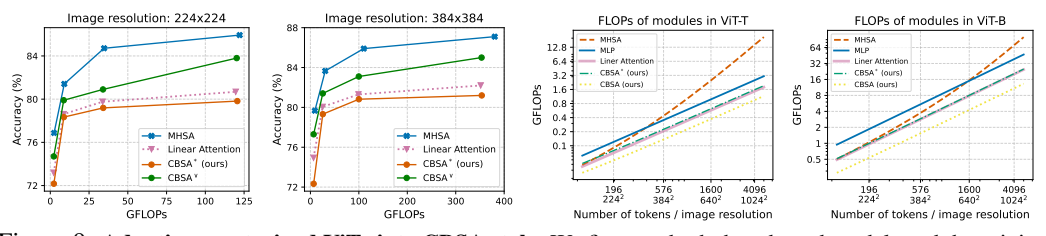


Figure 9: Adapting pre-trained ViTs into CBSA style. We finetune both the adapted models and the original ViTs on ImageNet-1K for 50 epochs, and report the top-1 accuracy on the validation set. CBSA* leverages the three distinct projection matrices inherited from the pretrained MHSA to calculate query, key, and value, instead of using a single projection matrix as in (8). CBSA* refers to CBSA* without the contraction step, which essentially becomes Agent Attention.

4.2 Evaluations on real-world visual tasks

We pretrain CBT models on the ImageNet-1K dataset, and finetune them on several downstream datasets. The top-1 accuracy on the validation sets is reported in Table 3. In particular, our CBT-

Small achieves comparable top-1 accuracy to ViT-S using only 30% of the parameters and 40% of the FLOPs. Compared to CRATE models built upon [16], our CBT models (with convolutional embedding layers) perform remarkably better while using fewer parameters and FLOPs.

We also conduct fair comparisons across different attention mechanisms, which can be regarded as variants of CBSA, and report the results as in Table 4. In this setting, our CBT models remain competitive with CRATE while computing significantly fewer pairwise similarities. These results confirm that, from MSSA to CBSA and then to TSSA, the number of pairwise similarity computations decreases at the cost of some performance. Throughput comparisons on high-resolution images (512×512) are presented in Table 7, showing that our method consistently achieves superior training and inference efficiency.

To investigate the potential of applying CBSA to large-scale pretraining, we preliminarily finetune ViT models pretrained on ImageNet-21K¹⁴ by adapting their attention blocks into the CBSA style. For comparison, we also adapt them into linear attention, with results shown in Fig. 9. Although CBSA deviates more from MHSA than linear attention and is consequently harder to adapt from pretrained ViTs, CBSA achieves performance comparable to linear attention with nearly the same FLOPs. Moreover, when adapted to Agent Attention, CBSA surpasses linear attention, which has been carefully experimented in [30].

For semantic segmentation, we build CBT decoders by stacking CBSA layers without feed-forward modules on top of ViT encoders, following the design of [31]. We evaluate them on the ADE20K dataset [43], with results shown in the left panel of Fig. 8. Our CBT decoder consistently surpasses both white-box (DEPICT) and black-box (Segmenter) counterparts that rely on softmax attention. In particular, the best-performing CBT decoder improves upon Segmenter by 1.5% mIoU while using only 20% of the FLOPs and 0.06% of the pairwise similarities in the decoder.

5 Related work

Efficient attention mechanisms can be roughly divided into two categories: sparse attention and linear attention [44]. Sparse attention approaches sparsify the attention matrix proactively by restricting the attention span to random, fixed [45, 19], learnable [46, 47] patterns, or their combinations. Linear attention [20, 48] decomposes the attention matrix into a product of two low-rank matrices and thus avoids its explicit computation via the associative property of multiplication. The idea of using representative tokens has been applied to both. Global tokens or memory can be introduced in sparse attention to maintain global connectivity, thereby further shrinking the attention span [49, 50]. Meanwhile, various works are implicitly sparse for reducing the number of input tokens [51, 52, 53, 54]. Agent tokens [30] and landmarks [28] can also be incorporated into linear attention from different perspectives.

Our CBSA distinguishes itself from previous efficient attention mechanisms by being inherently interpretable and derived from an optimization objective that efficiently compresses input tokens toward low-dimensional structures. Moreover, it can not only be viewed as sparse attention or linear attention through the representatives, but also mathematically generalizes linear attention and channel attention as special cases.

6 Conclusion

We proposed an optimization objective that compresses all input tokens by contracting a small number of representatives, thereby unifying the investigation towards interpretability and efficiency. By unrolling the gradient optimization steps for this objective, we derived an inherently interpretable and efficient attention mechanism, called CBSA. We found that many existing attention mechanisms can be generalized within the CBSA framework by specifying the number and structure of representatives, thus revealing their fundamental connections. We further validated the effectiveness of CBSA through extensive experiments on visual tasks. Therefore, we demonstrated that the preliminary framework established in this work offers a promising direction for exploring new attention mechanisms in an interpretable and efficient way.

¹⁴The checkpoint is obtained from the timm [42] library.

References

- [1] Ashish Vaswani, Noam Shazeer, Niki Parmar, Jakob Uszkoreit, Llion Jones, Aidan N. Gomez, Lukasz Kaiser, and Illia Polosukhin. Attention is all you need. In *NIPS*, pages 5998–6008, 2017.
- [2] Alexey Dosovitskiy, Lucas Beyer, Alexander Kolesnikov, Dirk Weissenborn, Xiaohua Zhai, Thomas Unterthiner, Mostafa Dehghani, Matthias Minderer, Georg Heigold, Sylvain Gelly, Jakob Uszkoreit, and Neil Houlsby. An image is worth 16x16 words: Transformers for image recognition at scale. In *ICLR*. OpenReview.net, 2021.
- [3] Kaiming He, Xinlei Chen, Saining Xie, Yanghao Li, Piotr Dollár, and Ross B. Girshick. Masked autoencoders are scalable vision learners. In *CVPR*, pages 15979–15988. IEEE, 2022.
- [4] Jacob Devlin, Ming-Wei Chang, Kenton Lee, and Kristina Toutanova. BERT: pre-training of deep bidirectional transformers for language understanding. In *NAACL-HLT (1)*, pages 4171–4186. Association for Computational Linguistics, 2019.
- [5] Alec Radford, Jeff Wu, Rewon Child, David Luan, Dario Amodei, and Ilya Sutskever. Language models are unsupervised multitask learners. 2019.
- [6] John Jumper, Richard Evans, Alexander Pritzel, Tim Green, Michael Figurnov, Olaf Ronneberger, Kathryn Tunyasuvunakool, Russ Bates, Augustin Žídek, Anna Potapenko, et al. Highly accurate protein structure prediction with alphafold. *nature*, 596(7873):583–589, 2021.
- [7] Mathilde Caron, Hugo Touvron, Ishan Misra, Hervé Jégou, Julien Mairal, Piotr Bojanowski, and Armand Joulin. Emerging properties in self-supervised vision transformers. In *ICCV*, pages 9630–9640. IEEE, 2021.
- [8] Tom B. Brown, Benjamin Mann, Nick Ryder, Melanie Subbiah, Jared Kaplan, Prafulla Dhariwal, Arvind Neelakantan, Pranav Shyam, Girish Sastry, Amanda Askell, Sandhini Agarwal, Ariel Herbert-Voss, Gretchen Krueger, Tom Henighan, Rewon Child, Aditya Ramesh, Daniel M. Ziegler, Jeffrey Wu, Clemens Winter, Christopher Hesse, Mark Chen, Eric Sigler, Mateusz Litwin, Scott Gray, Benjamin Chess, Jack Clark, Christopher Berner, Sam McCandlish, Alec Radford, Ilya Sutskever, and Dario Amodei. Language models are few-shot learners. In NeurIPS, 2020.
- [9] Daquan Zhou, Bingyi Kang, Xiaojie Jin, Linjie Yang, Xiaochen Lian, Zihang Jiang, Qibin Hou, and Jiashi Feng. Deepvit: Towards deeper vision transformer. *arXiv preprint arXiv:2103.11886*, 2021.
- [10] Yihe Dong, Jean-Baptiste Cordonnier, and Andreas Loukas. Attention is not all you need: pure attention loses rank doubly exponentially with depth. In *ICML*, volume 139 of *Proceedings of Machine Learning Research*, pages 2793–2803. PMLR, 2021.
- [11] Tianyu Guo, Druv Pai, Yu Bai, Jiantao Jiao, Michael I Jordan, and Song Mei. Active-dormant attention heads: Mechanistically demystifying extreme-token phenomena in llms. *arXiv preprint arXiv:2410.13835*, 2024.
- [12] Quoc-Vinh Lai-Dang. A survey of vision transformers in autonomous driving: Current trends and future directions. *arXiv preprint arXiv:2403.07542*, 2024.
- [13] Iz Beltagy, Matthew E Peters, and Arman Cohan. Longformer: The long-document transformer. *arXiv* preprint arXiv:2004.05150, 2020.
- [14] Ze Liu, Han Hu, Yutong Lin, Zhuliang Yao, Zhenda Xie, Yixuan Wei, Jia Ning, Yue Cao, Zheng Zhang, Li Dong, Furu Wei, and Baining Guo. Swin transformer V2: scaling up capacity and resolution. In *CVPR*, pages 11999–12009. IEEE, 2022.
- [15] Lemeng Wu, Xingchao Liu, and Qiang Liu. Centroid transformers: Learning to abstract with attention. arXiv preprint arXiv:2102.08606, 2021.
- [16] Yaodong Yu, Sam Buchanan, Druv Pai, Tianzhe Chu, Ziyang Wu, Shengbang Tong, Benjamin D. Haeffele, and Yi Ma. White-box transformers via sparse rate reduction. In *NeurIPS*, 2023.
- [17] Hubert Ramsauer, Bernhard Schäfl, Johannes Lehner, Philipp Seidl, Michael Widrich, Lukas Gruber, Markus Holzleitner, Thomas Adler, David P. Kreil, Michael K. Kopp, Günter Klambauer, Johannes Brandstetter, and Sepp Hochreiter. Hopfield networks is all you need. In *ICLR*. OpenReview.net, 2021.
- [18] Cynthia Rudin. Stop explaining black box machine learning models for high stakes decisions and use interpretable models instead. *Nat. Mach. Intell.*, 1(5):206–215, 2019.

- [19] Rewon Child, Scott Gray, Alec Radford, and Ilya Sutskever. Generating long sequences with sparse transformers. arXiv preprint arXiv:1904.10509, 2019.
- [20] Angelos Katharopoulos, Apoorv Vyas, Nikolaos Pappas, and François Fleuret. Transformers are rnns: Fast autoregressive transformers with linear attention. In *ICML*, volume 119 of *Proceedings of Machine Learning Research*, pages 5156–5165. PMLR, 2020.
- [21] Ziyang Wu, Tianjiao Ding, Yifu Lu, Druv Pai, Jingyuan Zhang, Weida Wang, Yaodong Yu, Yi Ma, and Benjamin D Haeffele. Token statistics transformer: Linear-time attention via variational rate reduction. *arXiv preprint arXiv:2412.17810*, 2024.
- [22] Yaodong Yu, Kwan Ho Ryan Chan, Chong You, Chaobing Song, and Yi Ma. Learning diverse and discriminative representations via the principle of maximal coding rate reduction. In *NeurIPS*, 2020.
- [23] Jie Hu, Li Shen, and Gang Sun. Squeeze-and-excitation networks. In *CVPR*, pages 7132–7141. Computer Vision Foundation / IEEE Computer Society, 2018.
- [24] Sanghyun Woo, Jongchan Park, Joon-Young Lee, and In So Kweon. CBAM: convolutional block attention module. In ECCV (7), volume 11211 of Lecture Notes in Computer Science, pages 3–19. Springer, 2018.
- [25] Yi Ma, Harm Derksen, Wei Hong, and John Wright. Segmentation of multivariate mixed data via lossy data coding and compression. *IEEE Trans. Pattern Anal. Mach. Intell.*, 29(9):1546–1562, 2007.
- [26] Peng Wang, Huikang Liu, Druv Pai, Yaodong Yu, Zhihui Zhu, Qing Qu, and Yi Ma. A global geometric analysis of maximal coding rate reduction. In ICML. OpenReview.net, 2024.
- [27] Kwan Ho Ryan Chan, Yaodong Yu, Chong You, Haozhi Qi, John Wright, and Yi Ma. Redunet: A white-box deep network from the principle of maximizing rate reduction. J. Mach. Learn. Res., 23:114:1–114:103, 2022.
- [28] Yunyang Xiong, Zhanpeng Zeng, Rudrasis Chakraborty, Mingxing Tan, Glenn Fung, Yin Li, and Vikas Singh. Nyströmformer: A nyström-based algorithm for approximating self-attention. In *AAAI*, pages 14138–14148. AAAI Press, 2021.
- [29] Amirkeivan Mohtashami and Martin Jaggi. Landmark attention: Random-access infinite context length for transformers. CoRR, abs/2305.16300, 2023.
- [30] Dongchen Han, Tianzhu Ye, Yizeng Han, Zhuofan Xia, Siyuan Pan, Pengfei Wan, Shiji Song, and Gao Huang. Agent attention: On the integration of softmax and linear attention. In *ECCV* (50), volume 15108 of *Lecture Notes in Computer Science*, pages 124–140. Springer, 2024.
- [31] Qishuai Wen and Chun-Guang Li. Rethinking decoders for transformer-based semantic segmentation: A compression perspective. In NeurIPS, 2024.
- [32] Nicolas Carion, Francisco Massa, Gabriel Synnaeve, Nicolas Usunier, Alexander Kirillov, and Sergey Zagoruyko. End-to-end object detection with transformers. In *ECCV (1)*, volume 12346 of *Lecture Notes in Computer Science*, pages 213–229. Springer, 2020.
- [33] Ehsan Elhamifar and René Vidal. Sparse subspace clustering. In CVPR, pages 2790–2797. IEEE Computer Society, 2009.
- [34] Emmanuel J Candes and Terence Tao. Decoding by linear programming. *IEEE transactions on information theory*, 51(12):4203–4215, 2005.
- [35] René Vidal, Yi Ma, and S. Shankar Sastry. *Generalized Principal Component Analysis*, volume 40 of *Interdisciplinary applied mathematics*. Springer, 2016.
- [36] Phillip Pope, Chen Zhu, Ahmed Abdelkader, Micah Goldblum, and Tom Goldstein. The intrinsic dimension of images and its impact on learning. *arXiv preprint arXiv:2104.08894*, 2021.
- [37] Duy-Kien Nguyen, Mahmoud Assran, Unnat Jain, Martin R Oswald, Cees GM Snoek, and Xinlei Chen. An image is worth more than 16x16 patches: Exploring transformers on individual pixels. *arXiv preprint arXiv:2406.09415*, 2024.
- [38] Feng Wang, Yaodong Yu, Guoyizhe Wei, Wei Shao, Yuyin Zhou, Alan Yuille, and Cihang Xie. Scaling laws in patchification: An image is worth 50,176 tokens and more. arXiv preprint arXiv:2502.03738, 2025.
- [39] Yunzhe Hu, Difan Zou, and Dong Xu. An in-depth investigation of sparse rate reduction in transformer-like models. In *NeurIPS*, 2024.

- [40] Robin Strudel, Ricardo Garcia Pinel, Ivan Laptev, and Cordelia Schmid. Segmenter: Transformer for semantic segmentation. In *ICCV*, pages 7242–7252. IEEE, 2021.
- [41] Yaodong Yu, Tianzhe Chu, Shengbang Tong, Ziyang Wu, Druv Pai, Sam Buchanan, and Yi Ma. Emergence of segmentation with minimalistic white-box transformers. *arXiv* preprint arXiv:2308.16271, 2023.
- [42] Ross Wightman. Pytorch image models. https://github.com/rwightman/pytorch-image-models, 2019.
- [43] Bolei Zhou, Hang Zhao, Xavier Puig, Tete Xiao, Sanja Fidler, Adela Barriuso, and Antonio Torralba. Semantic understanding of scenes through the ADE20K dataset. *Int. J. Comput. Vis.*, 127(3):302–321, 2019.
- [44] Yutao Sun, Zhenyu Li, Yike Zhang, Tengyu Pan, Bowen Dong, Yuyi Guo, and Jianyong Wang. Efficient attention mechanisms for large language models: A survey. arXiv preprint arXiv:2507.19595, 2025.
- [45] Niki Parmar, Ashish Vaswani, Jakob Uszkoreit, Lukasz Kaiser, Noam Shazeer, Alexander Ku, and Dustin Tran. Image transformer. In *International conference on machine learning*, pages 4055–4064. PMLR, 2018.
- [46] Yi Tay, Dara Bahri, Liu Yang, Donald Metzler, and Da-Cheng Juan. Sparse sinkhorn attention. In *ICML*, volume 119 of *Proceedings of Machine Learning Research*, pages 9438–9447. PMLR, 2020.
- [47] Aurko Roy, Mohammad Saffar, Ashish Vaswani, and David Grangier. Efficient content-based sparse attention with routing transformers. *Trans. Assoc. Comput. Linguistics*, 9:53–68, 2021.
- [48] Krzysztof Marcin Choromanski, Valerii Likhosherstov, David Dohan, Xingyou Song, Andreea Gane, Tamás Sarlós, Peter Hawkins, Jared Quincy Davis, Afroz Mohiuddin, Lukasz Kaiser, David Benjamin Belanger, Lucy J. Colwell, and Adrian Weller. Rethinking attention with performers. In *ICLR*. OpenReview.net, 2021.
- [49] Qipeng Guo, Xipeng Qiu, Pengfei Liu, Yunfan Shao, Xiangyang Xue, and Zheng Zhang. Star-transformer. In *NAACL-HLT (1)*, pages 1315–1325. Association for Computational Linguistics, 2019.
- [50] Manzil Zaheer, Guru Guruganesh, Kumar Avinava Dubey, Joshua Ainslie, Chris Alberti, Santiago Ontañón, Philip Pham, Anirudh Ravula, Qifan Wang, Li Yang, and Amr Ahmed. Big bird: Transformers for longer sequences. In *NeurIPS*, 2020.
- [51] Juho Lee, Yoonho Lee, Jungtaek Kim, Adam R. Kosiorek, Seungjin Choi, and Yee Whye Teh. Set transformer: A framework for attention-based permutation-invariant neural networks. In *ICML*, volume 97 of *Proceedings of Machine Learning Research*, pages 3744–3753. PMLR, 2019.
- [52] Sinong Wang, Belinda Z Li, Madian Khabsa, Han Fang, and Hao Ma. Linformer: Self-attention with linear complexity. arXiv preprint arXiv:2006.04768, 2020.
- [53] Wenhai Wang, Enze Xie, Xiang Li, Deng-Ping Fan, Kaitao Song, Ding Liang, Tong Lu, Ping Luo, and Ling Shao. Pyramid vision transformer: A versatile backbone for dense prediction without convolutions. In *ICCV*, pages 548–558. IEEE, 2021.
- [54] Yongming Rao, Wenliang Zhao, Benlin Liu, Jiwen Lu, Jie Zhou, and Cho-Jui Hsieh. Dynamicvit: Efficient vision transformers with dynamic token sparsification. In *NeurIPS*, pages 13937–13949, 2021.
- [55] Timothée Darcet, Maxime Oquab, Julien Mairal, and Piotr Bojanowski. Vision transformers need registers. In ICLR. OpenReview.net, 2024.
- [56] Dongchen Han, Xuran Pan, Yizeng Han, Shiji Song, and Gao Huang. Flatten transformer: Vision transformer using focused linear attention. In ICCV, pages 5938–5948. IEEE, 2023.
- [57] Xiangning Chen, Chen Liang, Da Huang, Esteban Real, Kaiyuan Wang, Hieu Pham, Xuanyi Dong, Thang Luong, Cho-Jui Hsieh, Yifeng Lu, and Quoc V. Le. Symbolic discovery of optimization algorithms. In NeurIPS, 2023.
- [58] Ilya Loshchilov and Frank Hutter. Decoupled weight decay regularization. In *ICLR (Poster)*. OpenReview.net, 2019.
- [59] Mark Everingham and John Winn. The pascal visual object classes challenge 2012 (voc2012) development kit. *Pattern Analysis, Statistical Modelling and Computational Learning, Tech. Rep*, 8(5):2–5, 2011.

Appendix

A Representative initialization

Besides pooling the input tokens, another intuitive choice for representative initialization is to set them as learnable (i.e., trainable) parameters, similar to the object queries in [32], the class embeddings in [40], and the registers in [55]. However, in this case we found that the attention matrix in the extraction (cross-attention) step 15 is extremely low rank. For example, although its maximal rank can be $m=p=\frac{d}{H}=64$ in CBT models, it typically remains around 5. This indicates that far fewer initialized representatives are being utilized than expected, leading to unsatisfactory performance of CBSA.

By contrast, when pooling-based initialization is employed, the rank of the attention matrix always attains its maximum, i.e., m. Nonetheless, as pointed out in [56], this still constitutes a low-rank bottleneck: linear attention underperforms softmax attention, whose attention matrix has rank $N \gg m$. Although this issue can be alleviated by introducing depth-wise convolution (DWC), which boosts performance while preserving linear complexity, our work does not involve this modification since we focus on theoretical contributions rather than empirical improvements.

B Derivations

Here, we show how (12) is derived by substituting $U_k^{\top}Q = L_k\Sigma_k$, $A_k = R_k$ into (7):

$$\sum_{k=1}^{K} \boldsymbol{U}_{k} \boldsymbol{L}_{k} \boldsymbol{\Sigma}_{k} \left(\mathbf{I}_{m} + \frac{m}{m\epsilon^{2}} (\boldsymbol{L}_{k} \boldsymbol{\Sigma}_{k})^{\top} (\boldsymbol{L}_{k} \boldsymbol{\Sigma}_{k}) \right)^{-1} \boldsymbol{R}_{k}^{\top}$$
(14)

$$= \sum_{k=1}^{K} \boldsymbol{U}_{k} \boldsymbol{L}_{k} \boldsymbol{\Sigma}_{k} \left(\boldsymbol{\mathbf{I}}_{m} + \frac{1}{\epsilon^{2}} \boldsymbol{\Sigma}_{k}^{\top} \boldsymbol{L}_{k}^{\top} \boldsymbol{L}_{k} \boldsymbol{\Sigma}_{k} \right)^{-1} \boldsymbol{R}_{k}^{\top}$$
(15)

$$= \sum_{k=1}^{K} \boldsymbol{U}_{k} \boldsymbol{L}_{k} \boldsymbol{\Sigma}_{k} \left(\boldsymbol{\mathbf{I}}_{m} + \frac{1}{\epsilon^{2}} \boldsymbol{\Sigma}_{k}^{2} \right)^{-1} \boldsymbol{R}_{k}^{\top}$$
(16)

$$= \sum_{k=1}^{K} \boldsymbol{U}_{k} \boldsymbol{L}_{k} \left(\boldsymbol{I}_{m} + \frac{1}{\epsilon^{2}} \boldsymbol{\Sigma}_{k}^{2} \right)^{-1} \boldsymbol{\Sigma}_{k} \boldsymbol{R}_{k}^{\top}$$
(17)

$$= \sum_{k=1}^{K} \boldsymbol{U}_{k} \boldsymbol{L}_{k} \left(\boldsymbol{I}_{m} + \frac{1}{\epsilon^{2}} \boldsymbol{\Sigma}_{k}^{2} \right)^{-1} \boldsymbol{L}_{k}^{\top} \boldsymbol{U}_{k}^{\top} \boldsymbol{Z}$$
(18)

$$= \sum_{k=1}^{K} \boldsymbol{U}_{k} F\left(\boldsymbol{L}_{k} \boldsymbol{\Sigma}_{k}^{2} \boldsymbol{L}_{k}^{\top}\right) \boldsymbol{U}_{k}^{\top} \boldsymbol{Z}$$

$$\tag{19}$$

$$= \sum_{k=1}^{K} \boldsymbol{U}_{k} F\left((\boldsymbol{U}_{k}^{\top} \boldsymbol{Z}) (\boldsymbol{U}_{k}^{\top} \boldsymbol{Z})^{\top}\right) \boldsymbol{U}_{k}^{\top} \boldsymbol{Z}$$
(20)

C More experimental results

Training setup. We train the CBT models in Table 3 and all models in Table 4 150 epochs with the Lion optimizer [57]. The learning rate is 2.0×10^{-4} , the weight decay coefficient is 0.05, and the batch size is 256. We also incorporate a warm-up strategy over the first 20 epochs. For data augmentation, we adopt a rather simple choice: just random cropping and random horizontal flipping. We apply label smoothing with a smoothing coefficient of 0.1. For fine-tuning, we use the AdamW optimizer [58], a learning rate of 5×10^{-5} , weight decay of 0.0 - 1, and batch size 64. The settings above are largely inherited from [16].

That is, rank (softmax $((\boldsymbol{U}_k^{ op} \boldsymbol{Z})^{ op} (\boldsymbol{U}_k \boldsymbol{Q}))$).

Quantitative segmentation properties. Following prior works [7, 41], we evaluate the zero-shot segmentation performance of ImageNet-1K pretrained models on the PASCAL VOC12 validation set [59]. Specifically, we assess the best-performing attention maps of the [CLS] token, but in a simplified setting that considers only three segmentation targets, instead of fine-grained semantic classes. In Table 5, we find that the hybrid model has consistently better segmentation performance. We also measure the segmentation performance of different layers in Table 6.

Table 5: **Zero-shot segmentation.** We use the jaccard similarity, which is also called intersection over union (IoU), to quantify the alignment between the [CLS] token's attention map and the segmentation ground truth. The best-performing results are highlighted in bold.

Segmentation target	(CRATE+CBT)-S	CRATE-S	CBT-S	ToST-S
Foreground Background	0.68 0.78	0.65 0.76	0.51 0.72	0.42 0.75
Boundary	0.18	0.17	0.15	0.12

Table 6: **Zero-shot segmentation across layers.** The top-performing three layers for each model are underlined.

Models	L1	L2	L3	L4	L5	L6	L7	L8	L9	L10	L11	L12
(CRATE+CBT)-S CRATE-S CBT-S	0.37 0.34 0.39	0.45	0.55 0.51 <u>0.43</u>		0.56 0.53 0.37	0.56	0.60 0.53 0.38	0.53 0.57 0.33	$\frac{0.59}{0.55}$ 0.35	0.56 0.52 0.34		0.55 0.39 0.33

Table 7: **Throughput comparisons.** The results below are experimented on the CIFAR-10 dataset with an image resolution of 512×512 .

im/sec	CBT-T	ViT-T	CRATE-T	ToST-T	CBT-S	ViT-S	CRATE-S	ToST-S
training inference			203 395	323 533				199 429

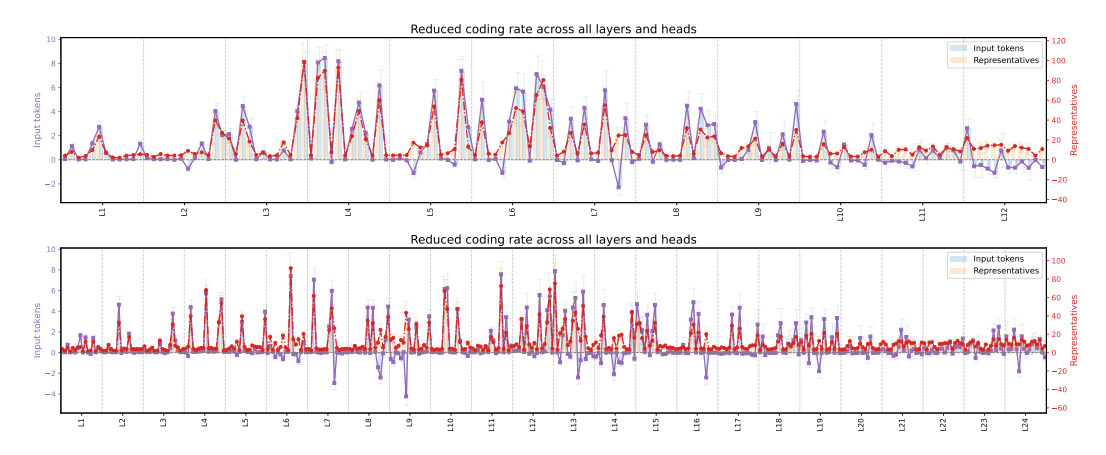


Figure 10: Additional results on CBT-B and CBT-L for the experiment in Fig. 6.

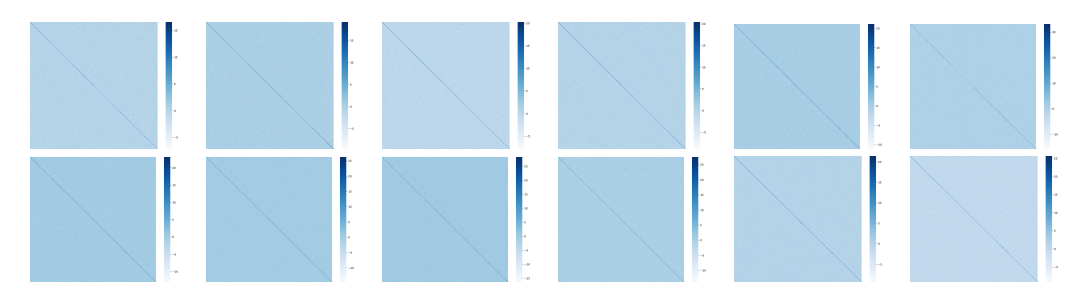


Figure 11: Gram matrices of basis vectors modeled by the layers of CBT-S. According to our assumption in Section 2, these matrices should approximate identity matrices.

D PyTorch implementation

Algorithm 1: PyTorch implementation of CBSA (8)

```
class CBSA(nn.Module):
      def __init__(self, dim, heads, dim_head):
          super().__init__()
          inner_dim = heads * dim_head
          self.heads = heads
          self.dim_head = dim_head
          self.scale = dim_head ** -0.5
          self.attend = nn.Softmax(dim=-1)
          self.pool = nn.AdaptiveAvgPool2d(output_size=(8, 8))
9
          # subspace bases
          self.proj = nn.Linear(dim, inner_dim, bias=False)
11
          # over-parameterization
12
          self.to_out = nn.Linear(inner_dim, dim)
13
          # step-sizes
          self.ss_x = nn.Parameter(torch.randn(heads, 1, 1))
          self.ss_rep = nn.Parameter(torch.randn(heads, 1, 1))
17
     def attention(self, query, key, value):
18
19
          dots = (query @ key.transpose(-1, -2)) * self.scale
          attn = self.attend(dots)
20
          out = attn @ value
21
          return out, attn
22
23
      def forward(self, x):
25
          b, n, c = x.shape
          height = width = int(n ** 0.5)
26
27
          # projection onto subspaces
          w = self.proj(x)
29
          # representative initialization
          rep = self.pool(w[:, :-1, :].reshape(b, height, width, c).
30
     permute(0, 3, 1, 2)).reshape(b, c, -1).permute(0, 2, 1)
          w = w.reshape(b, n, self.heads, self.dim_head).permute(0, 2,
          rep = rep.reshape(b, 64, self.heads, self.dim_head).permute(0,
32
      2, 1, 3)
          # representative extraction
33
          rep_delta, attn = self.attention(rep, w, w)
          rep = rep + self.ss_rep * rep_delta
          # representative contraction
36
37
          x_delta, _ = self.attention(rep, rep, rep)
          # contraction broadcast
          x_delta = attn.transpose(-1, -2) @ x_delta
          x_delta = self.ss_x * x_delta
          x_delta = rearrange(x_delta, 'b h n k -> b n (h k)')
41
          # projection back to the ambient space
42
          return self.to_out(x_delta)
```

Algorithm 2: PyTorch implementation of CBSA[†] in Fig. 8

```
class CBSA(nn.Module):
      def __init__(self, dim, heads, dim_head):
          super().__init__()
          inner_dim = heads * dim_head
          self.heads = heads
          self.dim_head = dim_head
          self.scale = dim_head ** -0.5
          self.attend = nn.Softmax(dim=-1)
9
          # subspace bases
          self.proj = nn.Parameter(self.scale * torch.randn(inner_dim,
10
      dim))
11
          # over-parameterization
          self.to_out = nn.Linear(inner_dim, dim)
12
          # step-sizes
          self.ss_x = nn.Parameter(torch.randn(heads, 1, 1))
          self.ss_rep = nn.Parameter(torch.randn(heads, 1, 1))
15
16
      \ensuremath{\mbox{def}} attention(self, query, key, value):
17
          dots = (query @ key.transpose(-1, -2)) * self.scale
          attn = self.attend(dots)
19
          out = attn @ value
20
21
          return out, attn
      def forward(self, x):
23
24
          b, n, c = x.shape
25
          # normalize the basis vectors
26
          proj = self.proj / self.proj.norm(dim=-1, keepdim=True)
          # projection onto subspaces
27
          w = rearrange(x @ proj.t(), 'b n (h k) -> b h n k', h=self.
28
     heads)
          # representative initialization (couple them with the basis
29
      vectors but preserved the norm)
          rep = rearrange(self.proj, '(h k) d -> h k d', h=self.heads)
30
          rep = rep 0 rearrange(proj, '(h k) d \rightarrow h k d', h=self.heads).
31
      transpose(-1, -2)
          rep = rep.expand(b, -1, -1, -1)
32
33
          # representative extraction
34
          rep_delta, attn = self.attention(rep, w, w)
          rep = rep + self.ss_rep * rep_delta
35
          # representative contraction
36
          x_delta, _ = self.attention(rep, rep, rep)
38
          # contraction broadcast
          x_delta = attn.transpose(-1, -2) @ x_delta
30
40
          x_delta = self.ss_x * x_delta
          x_delta = rearrange(x_delta, 'b h n k -> b n (h k)')
41
42
          # projection back to the ambient space
43
          return self.to_out(x_delta)
```

Algorithm 3: PyTorch implementation of CBSA* in Fig. 9

```
class CBSA(nn.Module):
      def __init__(
              self,
              dim: int,
              num_heads: int = 8,
              qkv_bias: bool = False,
              proj_bias: bool = True,
      ) -> None:
8
          super().__init__()
9
          assert dim % num_heads == 0, 'dim should be divisible by
10
      num_heads'
11
          self.num_heads = num_heads
          self.head_dim = dim // num_heads
12
          self.scale = self.head_dim ** -0.5
13
14
          self.pool = nn.AdaptiveAvgPool2d(output_size=(8, 8))
          self.qkv = nn.Linear(dim, dim * 3, bias=qkv_bias)
15
          self.proj = nn.Linear(dim, dim, bias=proj_bias)
16
17
18
      def attention(self, query, key, value):
19
          query = query * self.scale
          attn = query @ key.transpose(-2, -1)
20
21
          attn = attn.softmax(dim=-1)
          out = attn @ value
22
23
          return out, attn
24
25
      def forward(self, X: torch.Tensor) -> torch.Tensor:
          B, N, C = X.shape
26
          X_qkv = self.qkv(X).reshape(B, N, 3, C).permute(2, 0, 1, 3)
27
          X_q, X_k, X_v = X_qkv.unbind(0)
28
          H = W = int(N ** 0.5)
29
          Q = self.pool(X_q[:, :-1, :].reshape(B, H, W, C).permute(0, 3, ...)
30
       1, 2)).reshape(B, C, -1).permute(0, 2, 1)
          X_q = X_q.reshape(B, N, self.num_heads, self.head_dim).permute
31
      (0, 2, 1, 3)
          X_k = X_k.reshape(B, N, self.num_heads, self.head_dim).permute
      (0, 2, 1, 3)
          X_v = X_v.reshape(B, N, self.num_heads, self.head_dim).permute
      (0, 2, 1, 3)
          Q = Q.reshape(B, 64, self.num_heads, self.head_dim).permute(0,
34
      2, 1, 3)
          Q_delta, _ = self.attention(Q, X_k, X_v)
35
          Q = Q + Q_{delta}
36
          X_{delta}, _ = self.attention(Q, Q, Q)
37
38
          attn = ((X_q * self.scale) @ Q.transpose(-1, -2)).softmax(dim
      = -1)
          X = attn @ X_delta
39
          X = X.transpose(1, 2).reshape(B, N, C)
40
          X = self.proj(X)
41
42
          return X
```